

## Enhanced Localized Energetic-Ion Losses Resulting from Single-Pass Interactions with Alfvén Eigenmodes

X. Chen,<sup>1,\*</sup> M. E. Austin,<sup>2</sup> R. K. Fisher,<sup>3</sup> W. W. Heidbrink,<sup>1</sup> G. J. Kramer,<sup>4</sup> R. Nazikian,<sup>4</sup>  
D. C. Pace,<sup>3</sup> C. C. Petty,<sup>3</sup> and M. A. Van Zeeland<sup>3</sup>

<sup>1</sup>*University of California-Irvine, Irvine, California 92697, USA*

<sup>2</sup>*University of Texas-Austin, Austin, Texas 78712, USA*

<sup>3</sup>*General Atomics, P. O. Box 85608, San Diego, California 92186-5608, USA*

<sup>4</sup>*Princeton Plasma Physics Laboratory, P. O. Box 451, Princeton, New Jersey 08543, USA*

(Received 8 November 2012; published 7 February 2013; corrected 13 February 2013)

We report the first observation of prompt neutral beam-ion losses due to nonresonant scattering induced by toroidal and reversed shear Alfvén eigenmodes in the DIII-D tokamak. The coherent losses are of full energy beam ions expelled from the plasma on their first poloidal orbit. The first-orbit loss mechanism causes enhanced, concentrated losses on the first wall exceeding nominal levels of prompt losses. The loss amplitude scales linearly with the mode amplitude. The data provide a novel and direct measure of the radial excursion or scatter of particles induced by individual modes and may shed light on the mechanism for the scattering of energetic particles in interstellar medium.

DOI: [10.1103/PhysRevLett.110.065004](https://doi.org/10.1103/PhysRevLett.110.065004)

PACS numbers: 52.20.Dq, 52.35.Bj, 52.55.Fa, 52.70.Nc

In the ITER tokamak, it is essential that alpha particles from the D-T fusion reactions and injected 1 MeV deuterium neutral beam ions are thermalized in the plasma before being lost to the first wall. If sufficiently concentrated, escaping fast ions can damage the plasma facing components [1]. Indeed, damage to in-vessel components has already been observed due to losses induced by the interaction of radio frequency heated ions with multiple Alfvén eigenmodes (AEs) in the Tokamak Fusion Test Reactor (TFTR) [2]. Coil designs strive to maintain concentrated losses from magnetic field ripple below tolerable levels. In this Letter, we discuss a new mechanism that could concentrate fast-ion losses: modulation of barely confined fast-ion orbits by toroidal Alfvén eigenmodes (TAE) and reversed shear Alfvén eigenmodes (RSAE) leading to first-orbit neutral beam-ion losses. These interactions take place within one poloidal transit and can affect a wide region of the particle phase space, leading to enhanced coherent losses. This is in contrast to resonant losses that occur over narrow regions of phase space and over many poloidal transits of the particle. The new loss mechanism can account for a large fraction of fast ion losses observed in some DIII-D discharges and may potentially contribute to enhanced localized losses in ITER and future reactors.

Understanding the mechanisms of MHD induced fast ion transport and loss and validating theoretical models in present experiments is crucial for reliable predictions for ITER. AEs can redistribute fast ions in the plasma core through several mechanisms [1]. Flattening of the fast ion profile is caused by the combined action of many AEs [3–5], making theoretical predictions for ITER challenging. Existing experimental techniques cannot quantify the rate of transport caused by individual modes. Scintillator-based fast ion-loss detectors (FILD) observe resonant losses

when AEs transport confined fast ions across loss boundaries [6–8] but the size of the radial excursion is indeterminate. Profile flattening and loss bursts are observed during TAE avalanches but many modes act simultaneously at these events [9]. To test the modeling of AE fields and their impact on fast ion transport, an ideal experiment would detect the excursion caused by individual modes, much as a heavy ion beam probe measures field fluctuations [10]. In the experiments reported here, this limitation is overcome for the first time using discrete neutral beams to provide a known source of fast ions that complete a single poloidal orbit through the AE fields prior to their detection by a FILD. The magnitude of the oscillating prompt losses provides a direct measure of the radial “kick” (total radial displacement after one bounce orbit) imparted by each mode.

In addition to their importance for fusion research, direct measurements of the deflection of energetic particles by Alfvén waves can contribute to our understanding of natural plasmas. For example, short-wavelength Alfvén waves at rotational discontinuities scatter energetic particles in the interstellar medium [11], Alfvén waves cause pitch-angle scattering of cosmic rays [12], and Alfvén waves likely play a role in the acceleration of energetic ions in solar flares [13].

DIII-D has four pairs of neutral beam injectors (Fig. 1). The primary experiment (shot 146096) discussed here has a total of ~4.5 MW deuterium neutral beam power from combined coinjection (i.e., in the direction of the plasma current) of the 30L, 330L, and 330R beams. The 30L and 330L beams have identical geometry except for toroidal location. The primary fast ion loss diagnostic—a FILD [14] located toroidally at 165° near the midplane—is also shown on Fig. 1. The FILD obtains pitch and

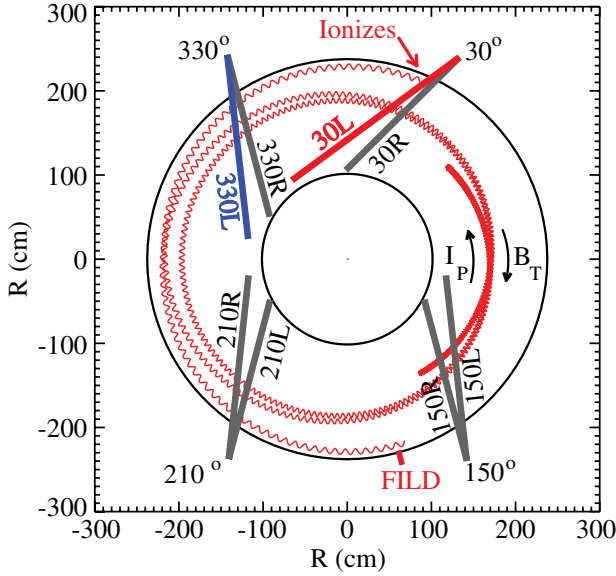


FIG. 1 (color online). Neutral beam injectors on DIII-D. The 30L and 330L neutral beams have identical geometry except for toroidal location. The near-midplane FILD is located at a toroidal angle of  $165^\circ$ . The orbit is the toroidal projection of the first poloidal transit of an ion that is born at the center of the 30L beam near the plasma edge.

energy resolved losses of beam ions with a bandwidth of 1 MHz.

Figure 2 shows time histories of key plasma parameters and loss measurements. Starting from  $t = 300$  ms into the discharge, the 330R beam injects continuously while the 30L and 330L beams are alternatively injected every 10 ms so that the total power is constant [Fig. 2(a)]. During the current ramp, the minimum safety factor ( $q_{\min}$ ) decreases from 4.9 to 2.1 [Fig. 2(b)], the toroidal field ( $B_T$ ) remains at 2.1 T, the central electron temperature ( $T_e$ ) rises from 0.6 to 1.4 keV, and the central density ( $n_e$ ) increases from  $1.2$  to  $2.0 \times 10^{13} \text{ cm}^{-3}$ . The continuous 330R beam together with the pulsed 30L and 330L beams drive a multitude of TAEs and frequency up-sweeping RSAEs with frequencies ranging from 50 to 220 kHz, as shown in the spectrogram of density fluctuations from interferometer signals [Fig. 2(c)]. Many of these modes also appear on the FILD spectrogram [Fig. 2(d)], indicating coherent beam ion losses induced by AEs.

Interestingly, the measured losses are source dependent and evolve with the  $q$  profile. Before 450 ms, the FILD only detects coherent losses during the 30L injection; after 450 ms, the losses coincide with injection of 330L. This is surprising given that the injection geometry for 30L and 330L beams are identical, apart from the difference in the toroidal locations. The continuous 330R beam has a different injection angle and does not contribute to the observed losses on the FILD. The coherent losses have similar pitch and energy as prompt losses produced by the 30L/330L beams in MHD-free plasmas. This source dependence is

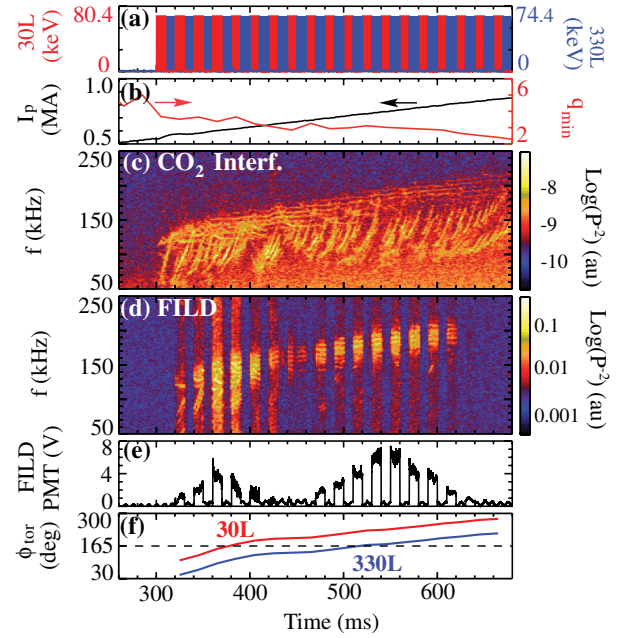


FIG. 2 (color online). Time evolution of (a) 30L (starts from 300 ms) and 330L (starts from 310 ms) power, (b) plasma current and  $q_{\min}$ , (c) smoothed FILD photomultiplier signal, and (f) toroidal location after first poloidal transit of ions born near the center of the 30L and 330L beams; spectrogram of cross power between vertical and radial  $\text{CO}_2$  interferometer chords (c) and spectrogram of FILD data (d) in a reversed magnetic shear plasma 146096.

because the unperturbed (no MHD activity) orbits of 30L and 330L beam ions reach different toroidal angles after one poloidal bounce and only the ones that closely approach the  $165^\circ$  FILD are deflected into the detector. Figure 1 shows the first bounce orbit of a 30L beam ion for the equilibrium at  $t = 365$  ms. A deuterium atom that ionizes near the plasma edge closely approaches the FILD after one poloidal bounce. If this unperturbed orbit starts from 330L, it will reach a smaller toroidal angle and miss the FILD. As the current increases, the unperturbed orbits of 30L beam ions move away from the FILD while those of 330L beam ions move in [Fig. 2(f)]. The closer to the FILD the unperturbed orbits of ions are born near the beam center (higher density), the stronger the loss signal is. The maximum loss amplitude [Fig. 2(e)] evolves during the current ramp—first peaking at 365 ms, then peaking again at 550 ms.

Examination of the FILD signal within a beam pulse confirms that coherent losses occur on the first bounce orbit. The calculated time for a full-energy ion to complete one poloidal drift orbit shown in Fig. 1 is  $\sim 80 \mu\text{s}$ . The time from the beam switch-on ( $10 \mu\text{s}$  resolution) to the FILD photomultiplier detects a loss signal is  $< 100 \mu\text{s}$ ; similarly, the loss signal decays after the beam pulse within  $100 \mu\text{s}$  (Fig. 3). The loss signal begins to oscillate at AE frequencies within one bounce period. This means that the

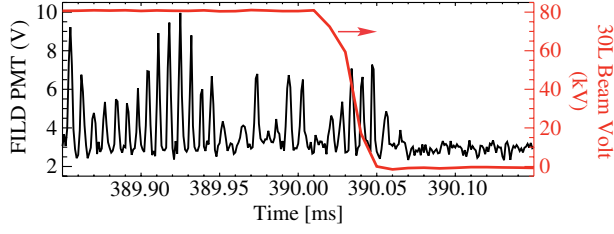


FIG. 3 (color online). The loss signal rapidly decreases when the corresponding neutral beam (voltage) turns off (consistent with a single poloidal transit period).

coherent losses commence before the beam ions have completed their first poloidal orbit. As resonant losses typically require interactions over multiple poloidal transits, this observation clearly indicates that the coherent loss is a prompt mechanism.

The AE-induced prompt losses reported here are commonly observed during co-injection in DIII-D plasmas over a range of plasma currents ( $0.5 < I_p < 1$  MA) and a range of densities ( $1.2 < n_e < 2.5 \times 10^{13} \text{ cm}^{-3}$ ). These losses are observed on the midplane FILD in circular-shaped (as presented here) and oval-shaped plasmas and also on the FILD [15] located  $\sim 45^\circ$  below the midplane. Although the FILD detects particles at the vessel wall, at low plasma current the ions first pass through the plasma core where the AE activity is localized. Therefore, core localized modes that contribute to coherent losses may be resolved better on the FILD detectors than on magnetic measurements.

The observed losses are dominated by trapped ions being scattered by AEs onto lost orbits that intersect the FILD. To illustrate this, in Fig. 4(a) we show a single particle that intersects a core RSAE and is lost to the FILD. The  $n = 2$  RSAE at 117 kHz is calculated using the ideal MHD code NOVA-K [16]. NOVA-K identifies an eigenmode by comparing the measured and simulated radial temperature fluctuation profiles and then scales the simulated amplitude to the measured one [17]. The interaction of the particle with the mode is calculated using the full-orbit SPIRAL code [18]. SPIRAL uses inputs such as the equilibrium reconstruction based on kinetic profiles, the beam ion deposition profile calculated by NUBEAM [19], and linear AEs from NOVA-K. The SPIRAL code computes Lorentz orbits with a realistic wall model. Coulomb scattering processes are included, although they have a minor effect on the prompt loss time scale. A neutral beam particle ionizes near the plasma edge on an unperturbed orbit that comes close to the FILD. When this ion traverses the plasma core in the presence of the RSAE, it is transported radially outward. The radial excursion depends on the phase of the mode. As the mode rotates, the radial excursion oscillates in and out, leading to coherent loss.

This process can also be viewed in the space described by the constants of motion of the unperturbed orbit.

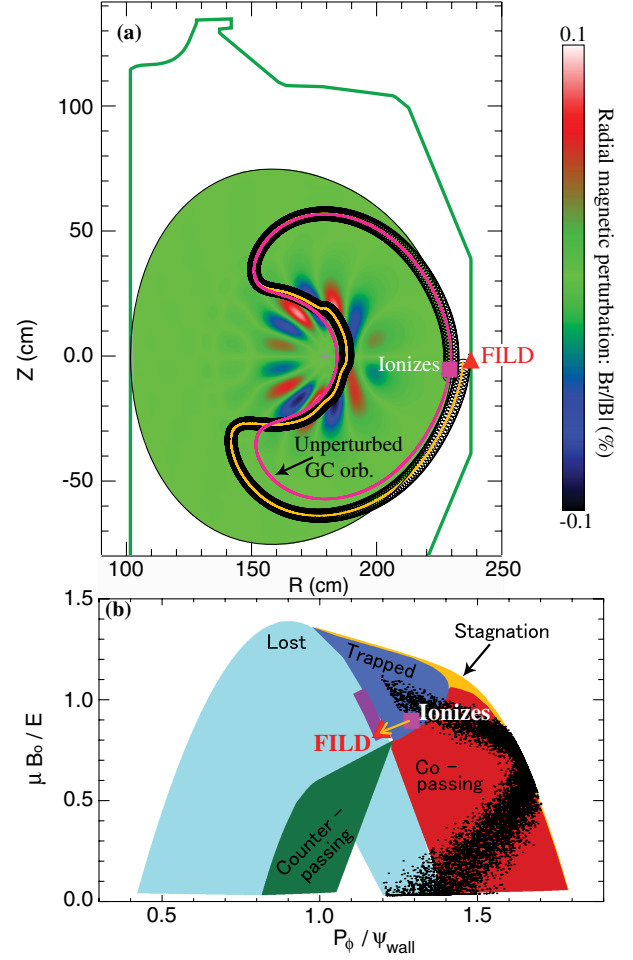


FIG. 4 (color online). (a) Orbits calculated using the SPIRAL code: guiding center (pink) orbit of a 30L beam ion (ionizes at pink square) in the absence of a mode; full (black) and guiding center (yellow) orbit lost to FILD (red triangle) in the presence of an  $n = 2$ , 117 kHz RSAE. (b) Classification of different orbit types in magnetic moment and canonical angular momentum space: lost, trapped, counter passing, co-passing, stagnation, and potato (intersection between trapped and co-passing). The 30L birth profile (black dots) is also shown. The orbits in the purple rectangular region reach the FILD within the detected pitch range at full energy. The start (pink square) and end (red triangle) of the perturbed orbit are marked in (a) and (b).  $B_0$  is the on-axis magnetic field;  $E = 80.4$  keV is the ion energy; and  $\psi_{\text{wall}}$  is the poloidal flux at the wall.

Figure 4(b) shows the calculated orbit topology [20] in terms of the magnetic moment  $\mu$  and canonical toroidal momentum  $P_\phi$  for ions with the full 30L injection energy of 80.4 keV for the equilibrium at  $t = 365$  ms. A wave can move an ion across the topological boundary between different types of orbits and cause radial transport. Particles that move towards smaller  $P_\phi$  values travel outward from the magnetic axis. The 30L beam ion density profile is plotted along with the range of orbits that could terminate at the FILD with the experimentally observed pitch. The equivalent start and end of the perturbed orbit

shown in Fig. 4(a) are also marked. The born trapped 30L beam ion is pushed across the loss boundary by the mode and lost to the FILD.

By tracking in time and frequency domain, the amplitudes of individual modes and the associated losses are obtained. The measured coherent losses ( $\Delta F$ ) show a linear dependence on the mode amplitude, indicating nondiffusive or ballistic loss but, as expected, the slope depends on the AE mode structure. Figure 5 compares  $\Delta F$  with the AE mode amplitude derived by electron-cyclotron-emission (ECE) electron temperature measurements ( $\delta T_e/T_e$ ) for an  $n = 2$  RSAE. The loss amplitude is proportional to the ionization rate at the birth location, and the radial kick imparted by a particular AE is proportional to the mode amplitude. Because of this relation, the data can be used to measure the radial kick caused by individual AE. Some prompt losses occur even in the absence of a mode because of the existence of unperturbed orbits that “connect” the FILD to the portion of phase space populated by injected neutrals. The amplitude of these unperturbed losses at the FILD ( $\bar{F}$ ) is proportional to the ionization rate where the orbit intersects the beam footprint. In the linear region, an AE at a higher (lower) amplitude gives the ions a larger (smaller) radial kick and effectively moves the birth location up (down) the ionization gradient, producing more (less) loss. Hence, the magnitude of the signal fluctuation ( $\Delta F$ ) is proportional to the ionization gradient (proportional to electron density gradient  $\partial n_e/\partial R$ ) and to the radial kick ( $\zeta$ ),

$$\Delta F/\bar{F} \approx \zeta(\partial n_e/\partial R)/n_e \quad \text{or} \quad \zeta \approx (\Delta F/\bar{F})L_n, \quad (1)$$

where  $L_n$  is the density scale length at the ionization point of the unperturbed prompt orbit. In practice,  $\bar{F}$  is the measured dc loss signal produced by the beam of interest,  $\Delta F$  is obtained from the fast Fourier transform at the mode frequency, and  $L_n$  is measured by Thomson scattering and profile reflectometry.

Using Eq. (1), with a mode amplitude of 1%, the calculated radial excursion is  $\sim 10$  cm caused by the example

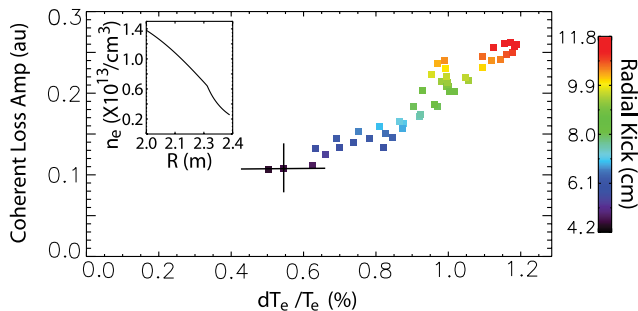


FIG. 5 (color online). Fluctuating FILD loss amplitude ( $\Delta F$ ) vs the mode amplitude for an  $n = 2$  RSAE at 52 kHz between 325 and 330 ms in discharge 146096 with edge density profile inserted (upper left). The radial kick ( $\zeta$ ) inferred from Eq. (1) is shown in the color contour.

$n = 2$  RSAE (at 52 kHz) (Fig. 5) and  $\sim 14$  cm by an  $n = 5$  TAE (at 120 kHz) existing at the same time.

Many experimental observations have been reproduced by SPIRAL simulations. Reverse full-orbit Monte Carlo SPIRAL simulations at different time windows during the current ramp are performed. Particles with full injection energy are introduced over the detected pitch range at a uniform rate for one AE cycle and traced from the FILD back to the simulated 30L and 330L beam detection planes over 50 AE cycles. Comparison of 30L and 330L beam footprint (pitch and height) from NUBEAM and the back-tracked particles shows good overlap with one beam but no overlap for the other. Losses are modulated at discrete mode phase relative to FILD (detection) or beam (ionization) consistent with experimentally observed modulated losses at AE frequencies. The majority of these ions are lost before completing their first orbit. Only a very small fraction ( $< 2\%$ ) get lost on later orbits (mostly on the second and third poloidal transitions). The calculated losses are coherent and scale linearly with mode amplitude, as observed experimentally. The radial kick is comparable to the measured kick.

In summary, four features of the measured fast ions expelled from the plasma—the pitch angle and gyroradius, the  $< 100 \mu\text{s}$  delay time, the toroidal-angle dependence vs plasma current, and the linear dependence on mode amplitude—show that the coherent FILD signals are produced by neutral beam ions that are deflected by AEs on their first bounce orbit. SPIRAL full orbit simulations confirm the interpretation. The enhanced losses are from co-injected neutral beam ions and nearly double the toroidally concentrated prompt losses at the FILD location. Since ITER will have off-axis co-injected 1 MeV beams, far edge trapped orbits that pass through the core could be susceptible to AE induced enhanced prompt loss. The potential impact on wall-loading thresholds should be considered.

These novel observations are also very important as a diagnostic technique. Presently, no major magnetic fusion facility can conclusively infer the radial excursion of fast ions imparted by individual modes in a well-defined time. We have shown that, by proper arrangement of a neutral beam injector and a FILD, such a determination is possible. Since many facilities have neutral beams and loss detectors, with proper adjustment of the toroidal displacement of the first orbits, or by utilizing a FILD array, this technique can be applied to measure the excursion produced by AEs and other instabilities. This will also provide a good test bed of the modeling of AE mode structures and of the fast-ion transport or loss they produced.

In addition, this work could shed light on a nonresonant mechanism that may lead to significant energetic particle transport such as in this case for fusion plasmas and possibly in astrophysical plasmas where large amplitude Alfvén waves can scatter particles.



This work was supported by the U.S. Department of Energy under Grants No. SC-G903402, No. DE-FG03-97ER54415, No. DE-FC02-04ER54698, and No. DE-AC02-09CH11466. The authors thank the DIII-D team for their support and B. A. Grierson and A. D. Turnbull for their help.

---

\*chenxi@fusion.gat.com

- [1] A. Fasoli *et al.*, *Nucl. Fusion* **47**, S264 (2007).
- [2] R. Nazikian, G. J. Kramer, C. Z. Cheng, N. N. Gorelenkov, H. L. Berk, and S. E. Sharapov, *Phys. Rev. Lett.* **91**, 125003 (2003).
- [3] W. W. Heidbrink *et al.*, *Phys. Rev. Lett.* **99**, 245002 (2007).
- [4] M. Ishikawa *et al.*, *Nucl. Fusion* **47**, 849 (2007).
- [5] F. Nabais, V. G. Kiptily, S. D. Pinches, and S. E. Sharapov, *Nucl. Fusion* **50**, 084021 (2010).
- [6] M. Garcia-Munoz *et al.*, *Phys. Rev. Lett.* **104**, 185002 (2010).
- [7] K. Ogawa, M. Isobe, K. Toi, F. Watanabe, D. A. Spong, A. Shimizu, M. Osakabe, S. Ohdachi, and S. Sakakibara, *Nucl. Fusion* **50**, 084005 (2010).
- [8] D. C. Pace, R. K. Fisher, M. García-Muñoz, W. W. Heidbrink, and M. A. Van Zeeland, *Plasma Phys. Controlled Fusion* **53**, 062001 (2011).
- [9] E. D. Fredrickson *et al.*, *Phys. Plasmas* **16**, 122 505 (2009).
- [10] T. P. Crowley, *IEEE Trans. Plasma Sci.* **22**, 291 (1994).
- [11] B. T. Tsurautani and C. M. Ho, *Rev. Geophys.* **37**, 517 (1999).
- [12] R. M. Kulsrud, *Plasma Physics for Astrophysics* (Princeton University, Princeton, NJ, 2005), Chap. 12.
- [13] J. C. Raymond, S. Krucker, R. P. Lin, and V. Petrosian, *Space Sci. Rev.* **173**, 197 (2012).
- [14] X. Chen, R. K. Fisher, D. C. Pace, M. Garcia-Munoz, J. A. Chavez, W. W. Heidbrink, and M. A. Van Zeeland, *Rev. Sci. Instrum.* **83**, 10D 707 (2012).
- [15] R. K. Fisher, D. C. Pace, M. Garcia-Munoz, W. W. Heidbrink, C. M. Muscatello, M. A. Van Zeeland, and Y. B. Zhu, *Rev. Sci. Instrum.* **81**, 10D 307 (2010).
- [16] N. N. Gorelenkov, C. Z. Cheng, and G. Y. Fu, *Phys. Plasmas* **6**, 2802 (1999).
- [17] M. A. Van Zeeland, G. J. Kramer, M. E. Austin, R. L. Boivin, W. W. Heidbrink, M. A. Makowski, G. R. McKee, R. Nazikian, W. M. Solomon, and G. Wang, *Phys. Rev. Lett.* **97**, 135001 (2006).
- [18] G. J. Kramer, R. V. Budny, A. Bortolon, E. D. Fredrickson, G. Y. Fu, W. W. Heidbrink, R. Nazikian, E. Valeo, and M. A. Van Zeeland, *Plasma Phys. Controlled Fusion* **55**, 025013 (2013).
- [19] A. Pankin, D. McCune, R. Andre, G. Bateman, and A. Kritz, *Comput. Phys. Commun.* **159**, 157 (2004).
- [20] M. A. Van Zeeland *et al.*, *Phys. Plasmas* **18**, 056114 (2011).